SAE INTERNATIONAL

A Simplified Design, Control and Power Management of Fuel Cell Vehicles

2014-01-1831
Published 04/01/2014

Ienkaran Arasaratnam
McMaster Univ.

CITATION: Arasaratnam, I., "A Simplified Design, Control and Power Management of Fuel Cell Vehicles," SAE Technical Paper 2014-01-1831, 2014, doi:10.4271/2014-01-1831.

Abstract

In the automotive industry, design processes always start with modeling and simulation for fast and cost-effective design prototype validation. Thereafter these simulations must be validated. Electric vehicles feature a wide range of components from different domains with controllers. One of the challenges in modeling and simulation of these vehicles lies in the integration of these diverse components into a single simulation environment. In this paper, an electric vehicle model is implemented along with an integrated hybrid storage system in MATLAB/Simulink. The hybrid energy storage system encompasses a proton exchange membrane (PEM) fuel cell system and a Lithium-ion battery, which are linked together via a current-regulated DC-DC converter. The simulated fuel cell vehicle model allows us to explore different power management strategies. Specifically, in order to improve the fuel cell stack efficiency and avoid damages to the fuel cell due to peak loads, a simple power-flow control strategy that allows us to operate the fuel cell on demand using a bypass contactor is evaluated. In order to validate the fuel cell vehicle model and demonstrate the effectiveness of the proposed power control strategy, numerous simulations are performed using highway drive cycles. Finally, the simulation results are compared with that of a traditional fuel cell vehicle model.

Introduction

Factors such as global warming, dwindling fossil fuel reserves, and energy security concerns combine to indicate that a replacement for the internal combustion engine vehicle is needed. Nowadays, alternative energy vehicles have become an attractive growth market. Fuel cell vehicles have the potential to address the problems surrounding the internal combustion engine vehicle without imposing any significant restrictions on vehicle performance, driving range, or fueling time. Toyota, Honda and Hyundai are all preparing to introduce fuel cell vehicles to market in the next few years. The fundamental concept of the fuel cell vehicle is excellent: it is highly efficient, does not have emissions, and the hydrogen fuel can be produced in the most efficient and economical location possible and moved to the desired location. However, there are some obstacles ahead of us to overcome before attaining the widespread commercialization of fuel cell vehicles, such as improvements in fuel cell and battery durability, development of a hydrogen infrastructure, reduction of high catalyst costs and improvements in getting power to wheels in a more efficient and cleaner way. Therefore, research on fuel cell vehicle design is imperative in order to improve vehicle performance and durability, increase efficiency and reduce costs.

In this paper, fuel cell vehicle simulation is created in the MAT-LAB/Simulink environment. In order to recuperate kinetic energy generated during braking, and prevent oxygen starvation resulting in damages to the fuel cell due to abrupt current demands, the fuel cell has to be paired up with a secondary storage system such as Lithium ion battery packs or ultracapacitor packs [20]. The addition of a secondary storage system offers numerous benefits to fuel cell vehicles. Specifically, it enables us to use a wide range of power/energy management strategies. In order to improve the fuel cell stack efficiency and to avoid damages to the fuel cell due to abrupt changes in loads, this paper implements a power-flow control strategy that enables the fuel cell to operate based on demand.

The remainder of this paper is organized as follows: Section II presents the modeling of fuel cells and Lithium ion batteries. Section III briefly reviews the half-bridge DC-DC converter used to interface the energy storage systems with E-motor electronics. Section IV presents an active power management configuration implemented in the fuel cell electric vehicle. To validate the effectiveness of the proposed fuel cell electric vehicle model and control strategies, computer simulations are performed using highway drive cycles in Section V. Section VI concludes the paper with remarks.

Modeling of Energy Storage Systems

In this paper, two types of energy storage systems, namely, fuel cells and Lithium ion batteries, are used for developing fuel cell electric vehicle simulation. In what follows, we describe the approaches taken to model these two storage systems.

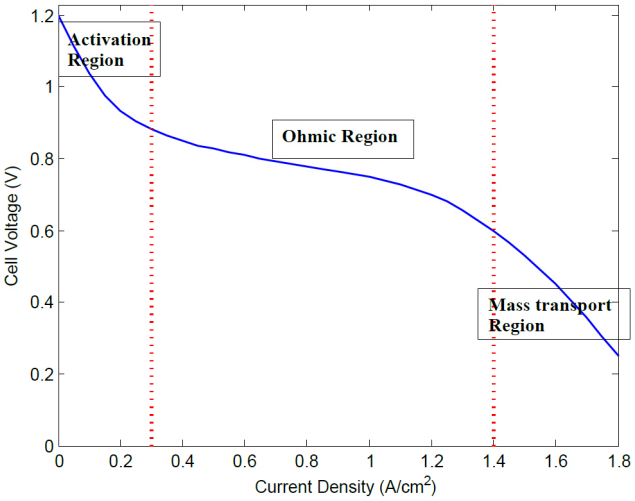

(a). Typical fuel cell polarization curve

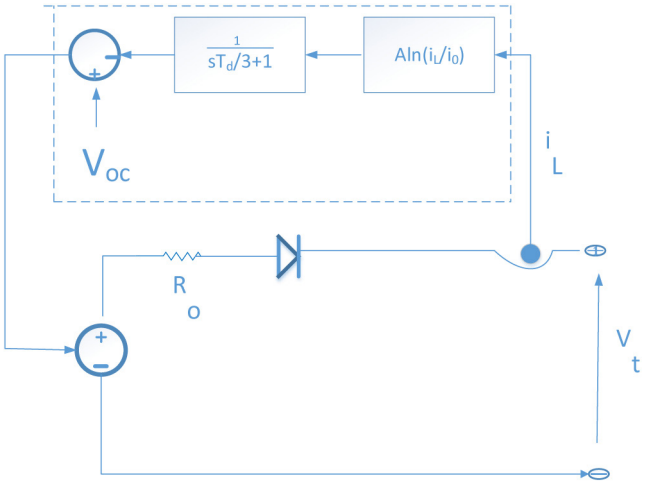

(b). Equivalent circuit model of the PEM fuel cell

Figure 1.

Proton Exchange Membrane Fuel Cells

Although there exist many types of fuel cells, Proton Exchange Membrane (PEM) fuel cells are widely used in electric vehicle development. Typically, PEM fuel cells consist of a membrane electrode assembly which is placed between two flow field plates. The membrane electrode assembly consists of two electrodes, namely, the anode and the cathode, each of which is coated with a thin platinum catalyst layer on one side and separated by a proton exchange membrane. The following overall cell reaction produces energy in PEM fuel cells:

$$H_{2(g)} + \frac{1}{2}O_{2(g)} \xrightarrow{Pt} H_2O \tag{1}$$

The basic building block for modeling a PEM fuel cell is a voltage-current polarization curve. As shown in Fig. 1(a), the polarization curve has three distinguishable regions [15]: activation region, ohmic region, and activation region (concentration) region. In the first (activation) region, the cell voltage drops rapidly due to energy lost in breaking and forming chemical bonds in the anode and cathode. In the second (ohmic) region, the cell voltage decreases linearly as the current increases. It arises from the resistance of the membrane and resistance between the electrode and the current collector. Finally, in the third (mass-transport) region, the voltage collapses sharply when current exceeds the upper limit of the safe operation. It represents mass transport losses resulting from the drop in the concentration of the reactants as they are consumed.

Fuel cells normally operate in the ohmic region and their operation in the mass transport region is avoided. For this reason, by ignoring the voltage drop due concentration loss, at steady state, the terminal voltage of the fuel cell, V_t, is written as follows:

$$\begin{aligned} V_t &= V_{oc} - V_{act.} - V_{ohm} \\ &= V_{oc} - \frac{1}{sT_d/3+1} A \ln \frac{I_L}{I_0} - R_o I_L, \end{aligned} \tag{2}$$

where T_d is the fuel cell response time in seconds, I_0 is the exchange current, R_o is the fuel cell resistance, I_L is the load current, and the slope of the Tafel curve A is given by $RT/(2\alpha F)$ (R is the ideal gas constant, T is the fuel cell operating temperature in Kelvin, α is the exchange current coefficient and F denotes the Faraday constant (96, 485 C mol^{-1})). The open circuit voltage of the fuel cell, V_{oc}, corresponding to the cell reaction (1) is described by the Nernst equation:

$$\begin{aligned} V_{oc} &= \text{Function}(T, \text{Partial Pres. of Species}) \\ &= E^0 + (T - T_0)\frac{\Delta S^0}{2F} + \frac{RT}{2F} \ln \frac{p_{H_2} p_{O_2}^{0.5}}{p_{H_2O}}, \end{aligned} \tag{3}$$

where E^0 denotes the standard thermodynamic voltage (1.229V), T_0 is the standard-state temperature (298.28K), ΔS^0 refers to the entropy of the chemical reaction (−44.43 J mol^{-1}K^{-1}) and pH_2,pO_2 and PH_2O denote the partial pressure of H_2, O_2 and H_2O in atm. Typically, PEM fuel cells operate at a fixed temperature of 353.15 K or 80 degree C and the partial pressure of the reactants is indirectly controlled by a PI control law to meet the required power demands [3,7]. Further description can be found in [14]. A similar model is also available in Matlab/simulink.

Lithium Ion Batteries

A battery model is required to capture battery chemistry accurately and to estimate its internal states, such as SOC (state-of-charge), SOH (state-of-health) and SOP (state-of-power). Battery modeling can be broadly categorized into two main categories:

- Equivalent electrical-circuit modeling and
- Electrochemical modeling

In this paper, a complete electrochemical model for a Lithium ion battery is adopted for its improved accuracy in responding to highly dynamic current demands [1]. As shown in Fig. 2, a Lithium ion electrochemical cell has three main domains- two composite electrodes (positive and negative) and a separator (see Fig. 2). For Lithium ion cells, the one-dimensional electrochemical model is known to capture relevant solid and electrolyte phase diffusion dynamics accurately. It also predicts the voltage response of current input. The state-space model of the battery comprises of a pair of equations: (i) The state equation describes the spatio-temporal evolution of the Lithium ion concentration $\mathbf{c}_s$ in the solid phase (ii) The measurement equation maps the state variable, $\mathbf{c}_s$, with the cell terminal voltage, V_t, as shown below:

$$\begin{aligned} \dot{\mathbf{c}}_s &= \mathbf{A}\mathbf{c}_s + \mathbf{B}I_L \\ V_t &= f(\mathbf{c}_s, I_L), \end{aligned}$$

where I_L is the load current, A and B are known matrices and $f(.,.)$ is a known nonlinear function. In practice, the concentration is estimated from the terminal voltage measurements using a Bayesian estimator. Moreover, the state-of-charge (SOC) is defined in terms of positive or negative electrode concentration[1]:

$$\text{SOC} = \frac{\bar{\varphi}_p - \varphi_{0,p}}{\varphi_{100,p} - \varphi_{0,p}},$$

where the normalized concentration

$$\varphi_p = \frac{c_{s,p}}{c_{s,p,\max}},$$

$\varphi_{0,p}$ and $\varphi_{100,p}$ are the normalized concentrations in the positive electrode when the cell is fully discharged and charged, respectively, and $\bar{\varphi}_p$ is a spherically-averaged concentration of the solid particle. Various electrochemical parameter values used to model the Lithium ion battery can be found in [1].

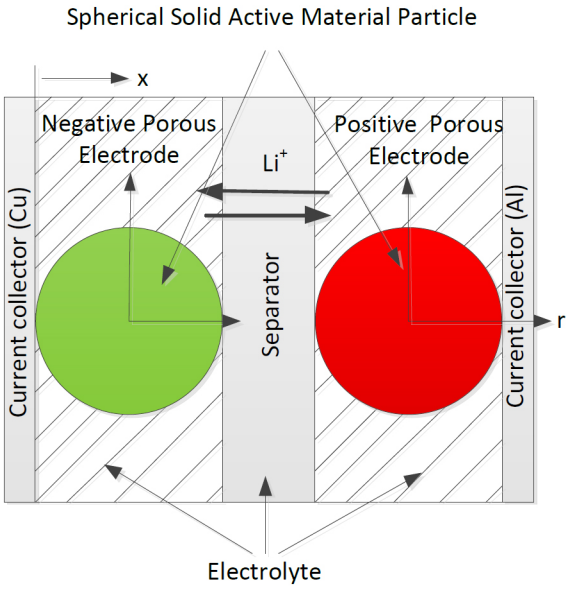

Figure 2. One Dimensional (x-direction) Electrochemical Cell Model

Half H-Bridge DC-DC Converters

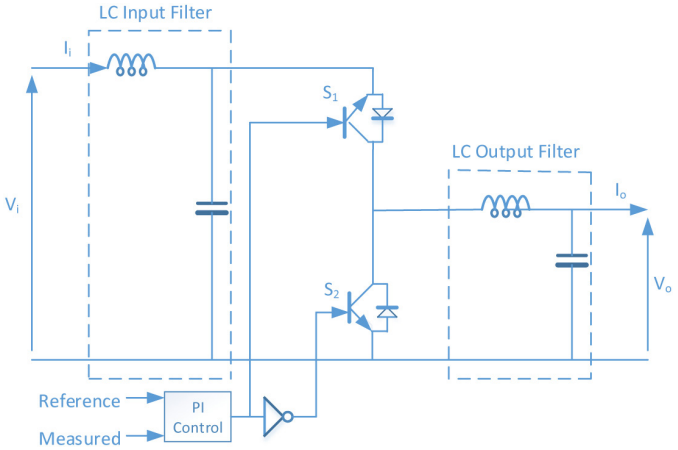

Figure 3. Bi-directional DC-DC Converter with PI Controller

Power electronics is the real enabler for hybrid energy storage systems. This paper implements a two-quadrant bi-directional DC-DC converter to interface hybrid energy sources with DC link/traction drive electronics [13, 5]. As shown in Fig. 3, it includes two IGBTs with antiparallel recovery diodes, forming a well known half H-bridge structure. The input and output LC filters are used to suppress rapid changes in voltage and current changes. The PI controller generates duty cycles for the IGBT switches based on the desired and measured inputs. Specifically, for the battery-fuel cell system, the PI controller regulates the fuel cell current.

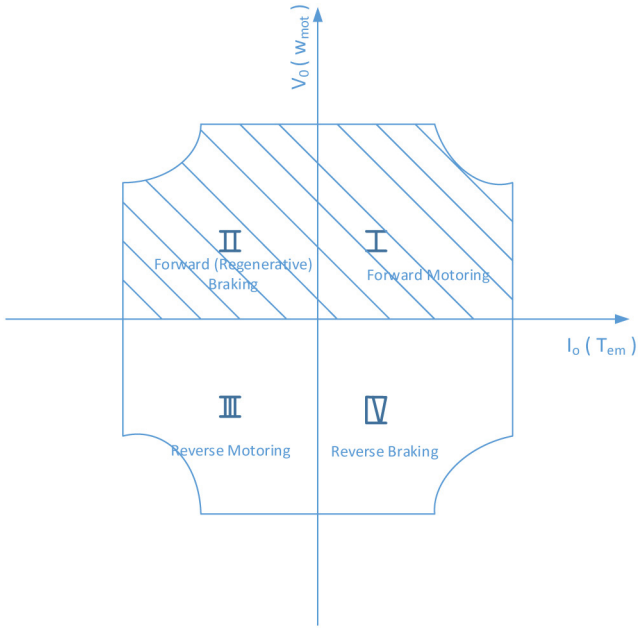

Figure 4. Four Quadrant Electrical (mechanical) Plane

In electric drive applications, a driven mechanical load has a specific set of requirements. The current(torque)-voltage(speed) possibilities of the electric drive can be represented by a graph consisting of four quadrants as shown in Fig. 4. The average value of the output voltage of a two-quadrant DC-DC converter is given by

$$V_o = DV_i,$$

where V_i and V_o are the input and output voltages of the DC-DC converter, respectively and D is the duty ratio for the IGBT switches. The average output current can be positive or negative.

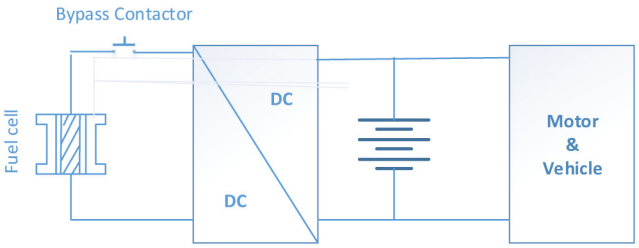

Figure 5. Active Configuration of Battery + Fuel cell System

- If $I_o > 0$, the E-motor will operate in a motoring mode and produce a positive electromagnetic torque (T_{em}) in a direction similar to the rotation speed ($\omega_{mot} > 0$). In this case, both the DC-DC converter and the E-motor operate in the first quadrant as denoted by (I) in the shaded region.
- During the E-motor operation with a positive speed ($\omega_{mot} > 0$), if the duty ratio is suddenly modified to decrease the DC output voltage, the average current through the E-motor changes the direction from that time instant. This negative current causes a negative electromagnetic torque opposing the rotational movement. Consequently, the E-motor operates in the regenerative braking mode as depicted in the second quadrant of the electrical (mechanical) plane.

Power Management

A power management strategy is crucial for properly controlling power flow from more than one energy storage systems, [9]. It should be able to provide high system efficiency, high performance, and protect its components. A number of different energy management configurations have been proposed in the literature for hybrid energy storage systems using the combinations of fuel cells, batteries and ultracapacitors [2, 8, 18]. In general, these configurations can be classified into two main types: Passive and active configurations.

This paper considers an active power management configuration. As shown in Fig. 5, the DC-DC power converter is placed in between the fuel cell and the battery to balance the power flow between them. An adaptive control strategy for active power sharing in the hybrid power source is achieved by adjusting the output current set-point of the fuel cell according to the power demand (see Fig. 6). Because highly abrupt loads damage fuel cells, a low-pass filter is included in the active configuration to ensure that the power of the fuel cell is smooth. In addition, a fuel cell bypass contactor is inserted to allow the fuel cell to operate only when the drive power demand exceeds an upper threshold (see Fig. 5). This idea was motivated by the fact that the fuel cell efficiency increases with high power output levels.

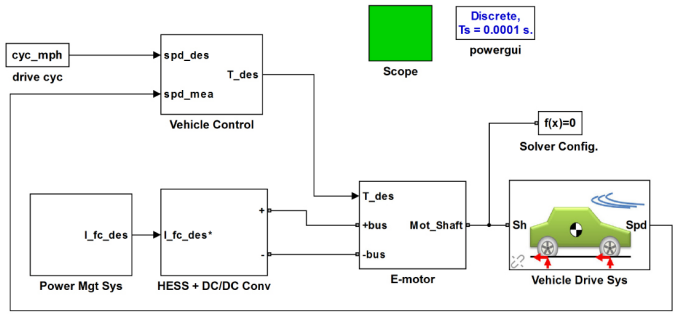

Figure 7. Top-level architecture of the battery-fuel cell vehicle model implemented in Matlab/Simulink

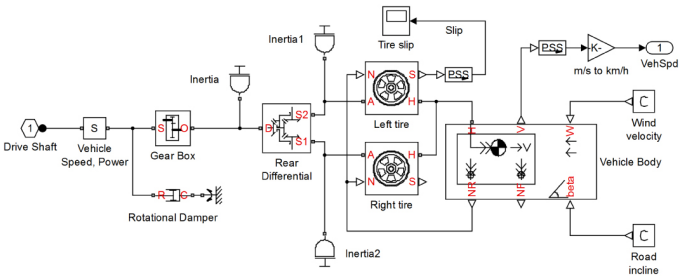

Figure 8. Matlab/Simulink block diagram of driveline-vehicle subsystem

Computer Experiments

Table 1.

Duration (s)	Distance travelled (km)	Average speed (km/h)	Maximum speed (km/h)
765	16.5	78	96.4

An overview of an electric vehicle model created in Matlab/Simulink is shown in Fig. 7. The vehicle model consists of five major subsystems- vehicle control(driver), power management, energy storage, E-motor and electronics and driveline. The vehicle control model senses actual vehicle speed and computes a speed error based on the instantaneous difference between this speed and the desired speed. The speed error is then processed by a PID control law to determine the desired motor torque, which is then fed to the E-motor drive. The power management subsystem ensures that the desired (electrical) power is available on the DC bus based on the drive power demand. The E-motor shaft feeds its output torque to the final driveline, the output of which is passed to the vehicle subsystem. The vehicle subsystem is further broken up into two major components- vehicle body dynamics and tire dynamics. The vehicle body block accepts the vehicle geometry, mass, aerodynamic drag and initial velocity to compute the normal load and feeds it to the tire dynamics. The tire dynamics accepts this normal load and the torque to compute a thrust force [10]. Vehicle speed is the output of the vehicle subsystem and fed back to the vehicle control subsystem. All of the driveline components are readily available as model libraries within the Matlab/Simulink environment [10].

In this study, we consider the HWFET (HighWay Fuel Economy Test) drive cycle as shown in Fig. 9(a). The HWFET cycle is a US dynamometer driving schedule used by vehicle manufacturers to determine fuel economy in highway driving conditions. Some of the HWFET cycle characteristics are tabulated in Table 1.

Vehicle speed and torque (both desired and measured) are shown in Figs. 9(a)-9(b). Overall, the model closely tracks the desired speed and torque traces without any significant deviations. The instantaneous speed error is less than 1 km/h.

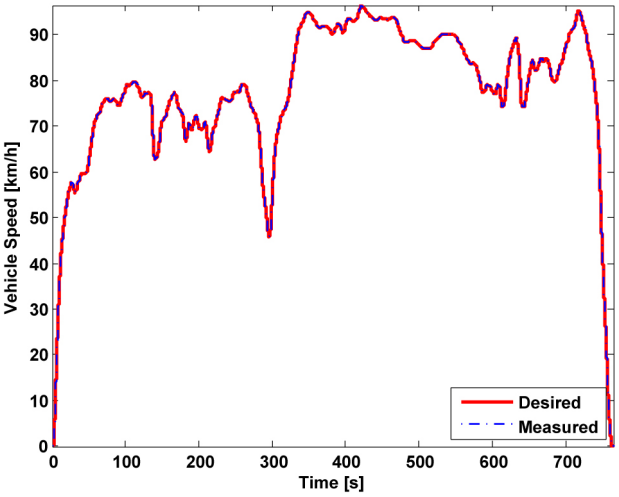

(a). Speed Profile

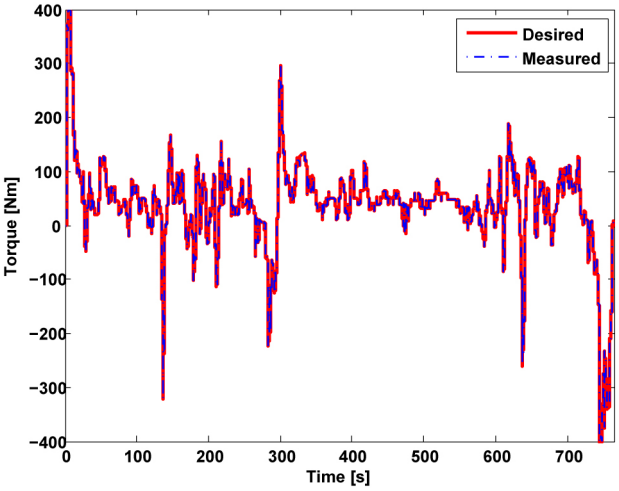

(b). Torque Profile

Figure 9. Speed and Torque Profiles (desired and measured)

The remainder of this section demonstrates the merits and demerits of the two different power management configurations-battery+FC (hybrid) systems with and without a fuel cell bypass contactor- considered in this paper. For the Battery+ Fuel cell system with the contactor, the contactor closes only when the drive power demand exceeds 5kW. Fig. 10(a) shows how the HWFET cycle drains the battery SOC. It is interesting to note that the fluctuations of the battery SOC has an inverse correlation with torque fluctuations as shown in Figs. 9(b)-10(a). The electrochemical model of the Li-ion battery makes it possible to respond to varying load demands instantaneously. The battery SOC drops more slowly in the case of the hybrid system without the contactor. On the other hand, for the hybrid system with the contactor, we can notice frequent SOC spikes and dips- whenever the contactor switches on and off, the demanded battery current changes accordingly affecting its SOC. Moreover, this situation is further exacerbated by the fact that fuel cells have a slow dynamic response during transients.

Fig. 10(b) shows a battery histogram. The statistical summary of this histogram is shown in Table 2. As expected, the battery draws less current in the hybrid system without the contactor than the system with the contactor. Since the fuel cell is up and running irrespective of drive power demands in the hybrid storage system without the contactor, the battery undergoes less stress. It indicates that the hybrid system with the contactor does not operate in favor of the battery; the battery lifespan in this system is expected to be shorter than that in the hybrid system without the contactor.

As shown in Table 3, unlike in the hybrid system without the contactor, for the hybrid system with the contactor, the fuel cell current is highly clustered in the vicinity of 15-25 A range. Moreover, for the hybrid system with the bypass contactor, the fuel cell stack efficiency improves significantly. As shown in Table 4, the improvement lies in the range of 2-3%. This can be attributed to the fact that fuel cells are known to operate with high efficiency at increased power demands [19].

Concluding Remarks

This paper presented an implementation of a simplified design, control and power management of fuel cell electric vehicles using Matlab/Simulink. It shows how the fuel cell model can be integrated with other energy storage systems (battery), mechanical systems and electrical systems Since a relatively simple configuration of power management strategy and control are used, the idea presented in this paper can be used as a perfect starting point for the design and control of fuel cell electrical vehicles. Moreover, it can be readily translated to make prototype fuel cell vehicles for educational demonstration purposes. Further research and prototyping will be needed in order to determine the scalability of this system to larger FCEVs. In order to meet different design specifications of OEMs (Original Equipment Manufacturers), various hybrid energy system topologies and advanced power/energy management strategies need to be investigated.

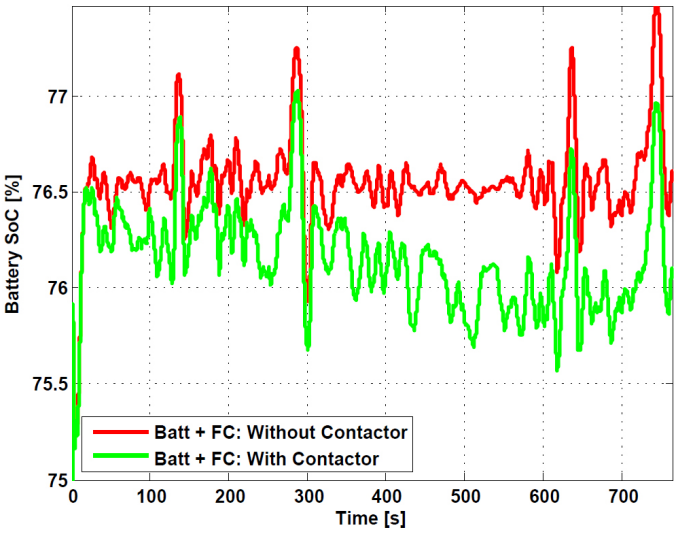

(a). Battery SoC

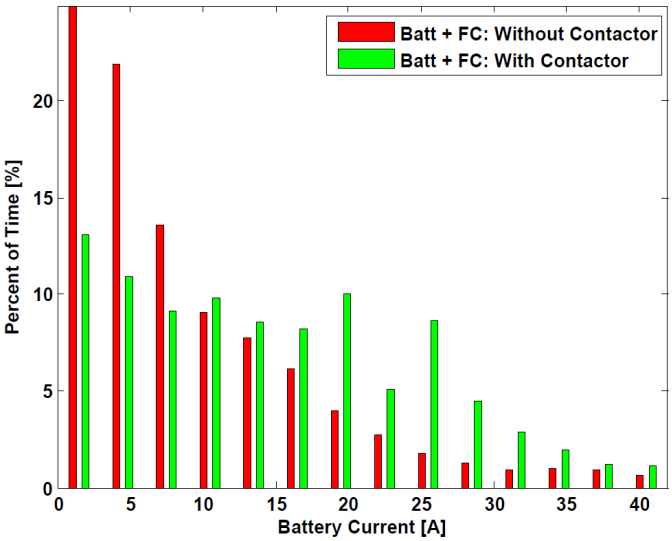

(b). Battery Current Histogram

Figure 10. Battery + Fuel Cell Vehicle

This paper also presented the merits and demerits of integrating a bypass contactor for power management. The energy management strategy presented in this paper is relatively simple. An interesting followup research topic could be to consider advanced strategies, as the direction of power flow has a huge impact on sizing, efficiency, and lifetime of hybrid storage systems. Li-ion batteries can also be coupled to a bank of high-power ultra-capacitors as this tandem setup reduces power-to-energy ratio of the battery and stress on both the battery and the fuel cell. Our simulation study assumes a fixed temperature distribution across the fuel cell and the battery. Another interesting future research work could be to add the thermal submodels of the the fuel cell and the battery models for a better representation of 'real' fuel cell vehicles.

Table 2.

Batt. Current	Without Contactor	With Contactor
Mean [A]	10.9	16.8
Std Dev [A]	12.7	13.6

Table 3.

FC Current	Without Contactor	With Contactor
Mean [A]	14.9	20.7
Std Dev [A]	7.8	4.3

Table 4.

Stack Efficiency	Without Contactor	With Contactor
Mean [%]	65.9	68.2
Std Dev [%]	0.8	0.6

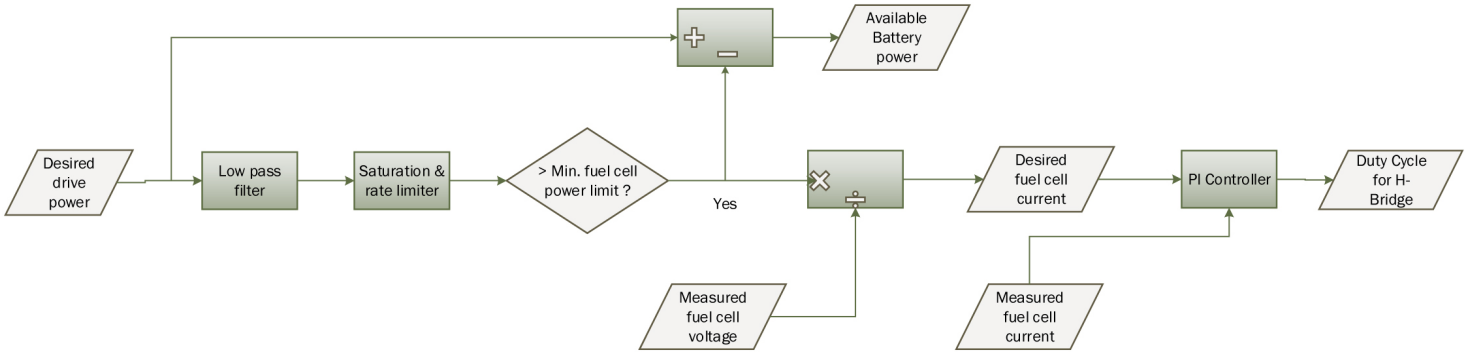

Figure 6. Adaptive Control Strategy for Battery + Fuel Cell Hybrid System

Table 5. Appendix A: Specification of Vehicle and HESS

Component	Parameter	Unit
Vehicle		
Mass	1200	kg
Frontal area	2.16	m^2
Drag Coefficient	0.26	
Tire radius	0.3	m
Tire rated vertical load	3000	N
Tire slip at peak force	6	%
Tire inertia	0.1	kgm^2
PEM Fuel Cell		
Voltage at 0A and 1A $[V_0, V_1]$	[400 380]	V
Nominal operating point [Inom, Vnom]	[285 300]	[A V]
Maximum operating point [Iend, Vend]	[347.3 288]	[A V]
Number of cells	400	
Nominal stack efficiency	57	%
Operating temperature	95	deg C
Nominal Air flow rate	1698	lpm
Nominal supply pressure [Fuel, Air]	[3 3]	bar
Nominal composition (%) [H2 O2 H2O(Air)]	[99.95 21 1]	%
Lithium ion Battery		
Initial SoC	0.75	
Nominal Voltage	185	V
No. cell in series	50	
No. cell in parallel	60	

References

1. Arasaratnam, I., Ahmed, R., El-Sayed, M., Tjong, J. et al., “Li-Ion Battery SoC Estimation Using a Bayesian Tracker,” SAE Technical Paper 2013-01-1530, 2013, doi:10.4271/2013-01-1530.
2. Bauman J. and Kazerani M., “A comparative study of fuelcell- battery, fuel-cell-ultracapacitor, and fuel-cell-battery-ultracapacitor vehicles”, *IEEE Transactions on Vehicular Technology*, 57(2), pp. 760769, March 2008.
3. Filho, C., “Modeling of a fuel cell/battery hybrid powertrain,” SAE Technical Paper 2008-36-0142, 2008, doi:10.4271/2008-36-0142.
4. Ehsani M., Gao Y., Gay S. E., and Emadi A., *Modern Electric, Hybrid Electric, and Fuel Cell Vehicles - Fundamentals, Theory, and Design*, First Edn, CRC Press, 2005.
5. Erickson R. and Maksimovic D., *Fundamentals of Power Electronics*, Kluwer Academic Publishers, USA, 2001.
6. Gao W., “Performance comparison of a hybrid fuel cell-Battery powertrain and a hybrid fuel cell-Ultracapacitor powertrain”, *IEEE Trans. Vehicular Tech.*, 54(3), pp. 846855, May 2005.
7. Larminie J. and Dicks A., *Fuel Cell Systems Explained*, John Wiley & Sons, 2002.
8. Lidozzi A. and Solero L., “Power balance control of multiple-input dc-dc power converter for hybrid vehicles,” *Proc. of IEEE International Symposium on Industrial Electronics*, 2(2):1467 1472, May 2004.
9. Luk P. C. K. and Rosario L. C., “Power and Energy Management of a Dual- Energy Source Electric Vehicle Policy Implementation Issues,” *Proc. Int'l Power Electronics and Motion Control Conf.*, pp. 1-6, Shanghai, China, 2006.
10. *Sim Driveline User's Guide*, R2012b, www.mathworks.com, Viewed on May 10-th 2013.
11. Miller J. M., *Propulsion System for Hybrid Vehicles*, 2004.
12. Miller J. M., Bohn T., Dougherty T.J. and Deshpande U., “Why hybridization of energy storage is essential for future hybrid, plug-in and battery electric vehicles,” *2009 IEEE Energy Conversion Congress and Exposition*, pp. 2614-2620, 2009.
13. Mohan N., Undeland T., Robbins W., *Power Electronics: Converters, Applications and Design*, 3rd Edn, John Willey & Sons Inc., USA, 2003.
14. Njoya S.M., Tremblay O., and Dessaint L., “A Generic Fuel Cell Model for the Simulation of Fuel Cell Vehicles,” *2009 IEEE Vehicle Power and Propulsion Conf.*, pp. 1722-1729, 2009.
15. Pukrushpan J. T., Stefanopoulou A. and Peng H., *Control of Fuel Cell Power Systems: Principles, Modeling, Analysis and Feedback Design*, Springer, 2004.
16. Schaltz E., *Design of a Fuel Cell Hybrid Electric Vehicle Drive System*, PhD Thesis, Dept. Energy Technology, Aalborg University, Denmark, Aug. 2010.
17. Schupbach R. M. and Balda J. C., “Comparing dc-dc Converters for Power Management in Hybrid Electric Vehicles,” *IEEE Int'l Electric Machines and Drives Conf.*, IEMDC03, Madison, WI, pp. 1369-1374, June 2003.
18. Thounthong P., Rael S., and Davat B., “Energy management of fuel cell/battery/supercapacitor hybrid power source for vehicle applications,” *J. Power Sources*, 193(1):376 385, Aug. 2009.

19. Thorstensen B., “A parametric study of fuel cell system efficiency under full and part load operation,” *J. Power Sources*, 92(2), pp. 916, Jan. 2001.
20. Vahidi A., Stefanopoulou A. and Peng H., “Model Predictive Control for Starvation Prevention in a Hybrid Fuel Cell System,” Proceeding of the 2004 American Control Conf., Boston, Massachusetts, June 30 - July 2, 2004.

The Engineering Meetings Board has approved this paper for publication. It has successfully completed SAE’s peer review process under the supervision of the session organizer. The process requires a minimum of three (3) reviews by industry experts.

ISSN 0148-7191

http://papers.sae.org/2014-01-1831